A PPV/MCM-41 Composite Material

Andras G. Pattantyus-Abraham and Michael O. Wolf*

Department of Chemistry, University of British Columbia, Vancouver, British Columbia, V6T 1Z1, Canada

Received December 10, 2003. Revised Manuscript Received March 12, 2004

Preparation of the conjugated polymer poly(1,4-phenylene vinylene) (PPV) inside the channels of the mesoporous silica MCM-41 is described. Polymerization was initiated inside the channels by deprotonated surface hydroxy groups. Presence of PPV was observed by infrared, absorption, and luminescence spectroscopy. A pore size reduction of 0.3 nm was seen in the composite material by nitrogen physisorption. A polymer mass content of 8% indicated the presence of approximately 3−6 polymer chains in each pore. Electron energy-loss spectroscopy of the composite revealed plasmon losses associated with the π-electron system on PPV. Energy-filtered transmission electron microscopy showed that the polymer was evenly distributed throughout the composite material through mapping of the π-electron plasmon losses.

Introduction

The discovery of electroluminescence in poly(1,4-phenylene vinylene) (PPV)[1] resulted in widespread interest in the electrooptical properties of conjugated polymers. In recent years, the encapsulation of such polymers has been the subject of scientific pursuit,[2−4] with the goal of measuring the electrical and optical properties of isolated conjugated polymer chains. Recent optical measurements on encapsulated polymers have allowed the intrachain energy transfer rate to be determined.[5,6] Encapsulation is also expected to protect the polymer chains from environmental degradation.

Many of the host properties desired for optimal conjugated polymer encapsulation can be found in self-assembled porous inorganic materials. These materials have been of longstanding scientific and industrial interest due to their large internal surface area, large sorption capacity, thermal stability, and catalytic activity toward small molecules.[7] Microporous materials (pore size < 2 nm), such as zeolites, have been used to encapsulate polypyrrole,[8] polythiophene,[9] and polyaniline.[10] Mesoporous materials (pore size 2−50 nm) can accommodate polymer chains with larger backbones, or possibly more than one chain per pore.

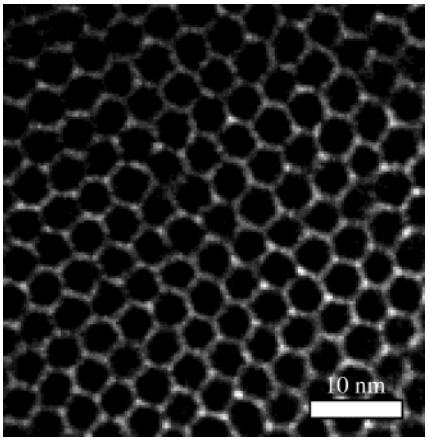

Figure 1. Transmission electron micrograph of MCM-41 material obtained using $C_{16}H_{33}(CH_3)_3NCl$ surfactant, showing hexagonal lattice spacing and wall thickness.

Among mesoporous materials, the siliceous material MCM-41 is of particular interest.[11,12] It shows uniform 1-D channels packed in a 2-D hexagonal array (Figure 1). This simultaneously endows the material with a large surface area (1000 $m^2\ g^{-1}$, almost all internal) and a large pore volume (0.8 $cm^3\ g^{-1}$). The straight channels ensure that the internal surface is readily accessible, which is ideal for both catalysis and molecular guest accommodation (over longer distances, 180° defects in channel direction are possible).

Mesoporous silica-based materials may be readily modified as there are many accessible surface hydroxy groups: it has been found that 26−30% of all Si atoms in MCM-41 bear a surface hydroxy group.[13] The surface

* To whom correspondence should be addressed. E-mail: mwolf@chem.ubc.ca.

(1) Burroughes, J. H.; Bradley, D. D. C.; Brown, A. R.; Marks, R. N.; Mackay, K.; Friend, R. H.; Burns, P. L.; Holmes, A. B. *Nature* **1990**, *347*, 539.
(2) Ozin, G. A.; Chomski, E.; Khushalani, D.; MacLachlan, M. J. *Curr. Opin. Colloid Interface Sci.* **1998**, *3*, 181.
(3) Moller, K.; Bein, T. *Chem. Mater.* **1998**, *10*, 2950.
(4) Cardin, D. J. *Adv. Mater.* **2002**, *14*, 553.
(5) Nguyen, T. Q.; Wu, J. J.; Doan, V.; Schwartz, B. J.; Tolbert, S. H. *Science* **2000**, *288*, 652.
(6) Tolbert, S. H.; Wu, J. J.; Gross, A. F.; Nguyen, T. Q.; Schwartz, B. J. *Microporous Mesoporous Mater.* **2001**, *44*, 445.
(7) van Bekkum, H., Flanigen, E. M., Jacobs, P. A., Jansen, J. C., Eds. *Introduction to Zeolite Science and Practice*; Elsevier: Amsterdam, The Netherlands, 2001; Vol. 137.
(8) Bein, T.; Enzel, P. *Angew. Chem., Int. Ed. Engl.* **1989**, *28*, 1962.
(9) Enzel, P.; Bein, T. *Chem. Commun.* **1989**, *18*, 1326.
(10) Enzel, P.; Bein, T. *J. Phys. Chem.* **1989**, *93*, 6270.
(11) Kresge, C. T.; Leonowicz, M. E.; Roth, W. J.; Vartuli, J.; Beck, J. S. *Nature* **1992**, *359*, 710.
(12) Beck, J. S.; Vartuli, J. C.; Roth, W. J.; Leonowicz, M. E.; Kresge, C. T.; Schmitt, K. D.; Wu, C. T.-W.; Olson, D. H.; Sheppard, E. W.; McCullen, S. B.; Higgins, J. B.; Schlenker, J. L. *J. Am. Chem. Soc.* **1992**, *114*, 10834.
(13) Landmesser, H.; Kosslick, H.; Storek, W.; Fricke, R. *Solid State Ionics* **1997**, *101*, 271.

10.1021/cm035303h CCC: $27.50
Published on Web 04/24/2004

derivatization can proceed by well-developed silane chemistry.[12,14] Additional functionality can be achieved by substituting other elements into the framework[15] and using organically modified framework sources.[2]

MCM-41, in its pure silica form, possesses many of the properties of an ideal host for conjugated polymers: it has narrow and aligned channels, with optically transparent and electrically insulating walls. Reports on polymer inclusion in MCM-41 appeared in the mid 1990s, involving polymers with both conjugated and nonconjugated backbones. In situ polymerization of aniline within the channels of MCM-41 was reported initially by Wu and Bein.[16] Acrylonitrile was polymerized similarly, using instead a solution of radical initiator.[17] Unger et al. prepared other free-radical initiated polymers in MCM-41: polystyrene, poly(methyl methacrylate), and polyvinyl acetate.[18] Soluble polymers prepared ex situ may also be introduced into the channels through simple diffusion.[19−21]

In general, the polymer distribution in these composite materials is inferred from indirect measurements, such as N_2 physisorption.[20] Diffraction techniques may be used in cases where there is contrast matching (electron density for X-ray diffraction,[22,23] neutron scattering cross-section for neutron diffraction[24,25]) with the walls of the host.

The presence of organic molecules within the channels of MCM-41 is difficult to establish by more direct means. The use of transmission electron microscopy (TEM) is limited by the low electron scattering cross-section of C and H; polymers containing heavier elements may be observed more readily.[23] Heavy-element staining of organic molecules is possible for certain functional groups[26] but may not provide sufficient contrast for small amounts of polymer. The host may also be etched away to observe the morphology of the polymer chains.[27] As such, the observation of organic polymer chains *inside* the channels of MCM-41 by TEM has not been reported. The use of high-resolution chemical analysis in the TEM, through electron energy-loss spectroscopy (EELS) and energy-filtered TEM (EFTEM), has not yet been explored in this context, although it has been used extensively to study polymer blends.[26,28−33] In this report, we follow an EFTEM-based approach first reported for chromophore mapping in biological specimens,[34−36] and show directly the presence of conjugated polymer chains in the channels of the MCM-41 host.

The introduction of PPV into MCM-41 must proceed through in situ synthesis because of the insoluble and infusible nature of the polymer. The polymerization of PPV can be carried out by numerous routes,[37] with the simplest being a base-initiated condensation known as the Gilch route.[38] However, this route was not exploitable within the MCM-41 host: although the monomer could be readily loaded into MCM-41 through sublimation, the subsequent introduction of a base of sufficient strength was not possible. Aqueous bases attacked and dissolved the host, and nonaqueous bases solubilized the monomer and extracted it from the pores before polymerization could occur. Other polymerization routes were investigated, and a solution to this problem was found through the work of Kumar et al.,[39] who had prepared PPV within the pores of Vycor, a disordered porous glass. This approach used a more reactive monomer, xylylene bis(tetrahydrothiophenium chloride), which could be polymerized by deprotonated surface hydroxy groups.

In similar fashion, MCM-41 was converted to a basic form by deprotonating its surface hydroxy groups with a nonaqueous base (tetrabutylammonium hydroxide (TBAOH) in MeOH) and isolated. This activated form of MCM-41 thus contained the initiating base within its channels. Polymer confinement occurred through the rapid polymerization of the monomers within the host channels (Figure 2).

Experimental Section

All chemicals were obtained from Aldrich Inc. Xylylene bis(tetrahydrothiophenium chloride) was purified by recrystallization from H_2O. EtOH was dried over 4A molecular sieves.

MCM-41 was synthesized according to a literature procedure using $CH_3(CH_2)_{15}N(CH_3)_3Cl$ as the surfactant.[40] The synthesis was carried out at 80 °C for 2 days in a Teflon-lined stainless steel bomb. After the collected powder was washed with MeOH and H_2O, it was calcined under air with a heating rate of 1 °C min^{-1} to 540 °C and held at that temperature for 6 h. N_2 adsorption analysis was performed on a Micromeritics ASAP 2010 instrument.

Thermogravimetric analysis was carried out using a TA Instruments TGA 51 under N_2 flow and a heating rate of 10 °C min^{-1}. Infrared spectra were obtained from KBr pellets

(14) Jaroniec, C. P.; Kruk, M.; Jaroniec, M.; Sayari, A. *J. Phys. Chem. B* **1998**, *102*, 5503.
(15) Sayari, A.; Liu, P. *Microporous Mater.* **1997**, *12*, 149.
(16) Wu, C.-G.; Bein, T. *Science* **1994**, *264*, 1757.
(17) Wu, C.-G.; Bein, T. *Science* **1994**, *266*, 1013.
(18) Llewellyn, P. L.; Ciesla, U.; Decher, H.; Stadler, R.; Schüth, F.; Unger, K. K. In *Zeolites and Related Microporous Materials: State of the Art 1994*, Garmisch-Partenkirchen, Germany, 1994; Weitkamp, J., Karge, H. G., Pfeifer, H., Hölderlich, W., Eds.; Elsevier: Amsterdam, The Netherlands, 1994; p 2013.
(19) Wu, J. J.; Gross, A. F.; Tolbert, S. H. *J. Phys. Chem. B* **1999**, *103*, 2374.
(20) Xi, H. G.; Wang, B. H.; Zhang, Y. B.; Qian, X. F.; Yin, J.; Zhu, Z. K. *J. Phys. Chem. Solids* **2003**, *64*, 2451.
(21) Wang, B. H.; Xi, H. A.; Yin, J.; Qian, X. F.; Zhu, Z. K. *Synth. Met.* **2003**, *139*, 187.
(22) Marler, B.; Oberhagemann, U.; Vortmann, S.; Gies, H. *Microporous Mater.* **1996**, *6*, 375.
(23) MacLachlan, M. J.; Aroca, P.; Coombs, N.; Manners, I.; Ozin, G. A. *Adv. Mater.* **1998**, *10*, 144.
(24) Tun, Z.; Mason, P. C. *Acta Crystallogr., Sect. A: Found. Crystallogr.* **2000**, *56*, 536.
(25) Ramsay, J. D. F. *Adv. Colloid Interface Sci.* **1998**, *77*, 13.
(26) Varlot, K.; Martin, J. M.; Quet, C. *Polymer* **2000**, *41*, 4599.
(27) Johnson, S. A.; Khushalani, D.; Coombs, N.; Mallouk, T. E.; Ozin, G. A. *J. Mater. Chem.* **1998**, *8*, 13.
(28) Horiuchi, S.; Yase, K.; Kitano, T.; Higashida, N.; Ougizawa, T. *Polym. J.* **1997**, *29*, 380.
(29) Brown, G. M.; Butler, J. H. *Polymer* **1997**, *38*, 3937.
(30) Du Chesne, A. *Macromol. Chem. Phys.* **1999**, *200*, 1813.
(31) Correa, C. A.; Hage, E. *Polymer* **1999**, *40*, 2171.
(32) Zhou, F.; Plies, E.; Keller, F.; Schurig, V. *J. Electron Microsc.* **1999**, *48*, 601.
(33) Horiuchi, S.; Ishii, Y. *Polym. J.* **2000**, *32*, 339.
(34) Barfels, M. M. G.; Jiang, X. G.; Heng, Y. M.; Arsenault, A. L.; Ottensmeyer, F. P. *Micron* **1998**, *29*, 97.
(35) Davis, J. A.; Heng, Y. M.; Barfels, M. M. G.; Bisland, S. K.; Gariepy, J.; Ottensmeyer, F. P. *J. Electron Microsc.* **2000**, *49*, 629.
(36) Ottensmeyer, F. P.; Davis, J. A.; Heng, Y. M.; Barfels, M. M. G. In *Microbeam Analysis 2000*, Kailua Kona, Hawaii, 2000; Williams, D. B.; Shimizu, R., Eds.; Institute of Physics Publishing: Bristol, 2000, p 181.
(37) Hsieh, B. R. *Poly(p*-phenylene vinylene)s: Methods of preparation and properties; Salamone, J. C., Ed.; CRC Press: Boca Raton, Fl, 1996; Vol. 9, p 6537.
(38) Gilch, H. G.; Wheelwright, W. L. *J. Polym. Sci., Part A: Polym. Chem.* **1966**, *4*, 1337.
(39) Kumar, D. N.; Bhawalkar, J. D.; Prasad, P. N. *Appl. Opt.* **1998**, *37*, 510.
(40) Khushalani, D.; Kuperman, A.; Coombs, N.; Ozin, G. A. *Chem. Mater.* **1996**, *8*, 2188.

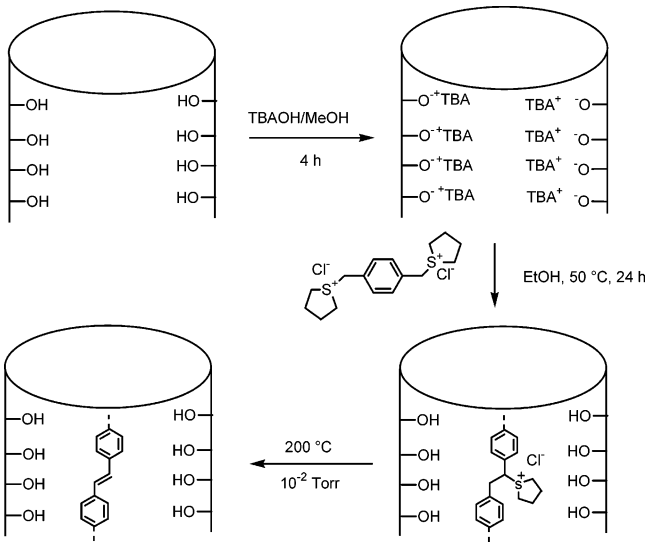

Figure 2. Synthetic scheme for the preparation of PPV/MCM-41 hybrid material. Only one chain is shown in the pore for clarity.

using a BOMEM MB155S FT-IR spectrometer. Powder X-ray diffraction patterns were collected on a Rigaku Rotaflex rotating-anode diffractometer.

Adapting the work of Kumar et al.,[39] the calcined MCM-41 was dried under vacuum at 100 °C and then treated with 1 M TBAOH in MeOH under a N_2 atmosphere. This mixture was left to stand for 4 h at room temperature, after which the basic MCM-41 was filtered off in a Schlenk filter and dried under vacuum. The resulting solid was transferred into a 10−20% w/w solution of xylylene bis(tetrahydrothiophenium chloride) in dry EtOH at 50 °C for 24 h, and then washed with EtOH and H_2O to remove excess monomer and base. The bright yellow-green powder was dried under vacuum at room temperature; subsequent heating to 200 °C under vacuum (10^{-2} Torr) for 6 h resulted in the powder turning bright yellow.

For TEM analysis, samples were deposited on lacey carbon-coated Cu grids (Ted Pella, Inc.) from a suspension in MeOH. EELS and EFTEM were carried out on a Tecnai F20 TEM equipped with a Gatan imaging filter (GIF). The accelerating voltage was 197 kV (200 kV nominally, offset by 3 kV by the GIF). Loss spectra were recorded in TEM mode by placing the particle of interest above the GIF entrance aperture (diameter 2.0 mm). The zero-loss peak was recorded separately for subtraction by moving to an empty area on the grid. The system energy resolution, given by the fwhm of the zero-loss peak, was 0.9 eV. The energy dispersion of the spectrometer was 0.10 eV/pixel, which was calibrated using a 50 eV wobble on the drift tube. EFTEM images were acquired with a 2 eV slit.

The UV/Vis absorbance spectrum was measured for PPV/MCM-41 as a Nujol mull pressed between quartz plates, using a Unicam UV-2 spectrometer. The room-temperature photoluminescence spectrum was measured with a Perkin-Elmer LS-5b spectrometer, using composite material deposited on a quartz plate from a suspension in MeOH. The excitation wavelength was 380 nm.

Results and Discussion

The pure silica MCM-41 host was synthesized following a literature procedure.[40] Characterization with X-ray diffraction and N_2 physisorption indicated substantial batch-to-batch variations in the lattice constant (4.3−4.5 nm) and BJH pore diameter (3.1−3.6 nm). Thus, comparisons were made only with materials prepared in the same batch. The BET surface area was 1.0×10^3 m^2 g^{-1}, and the total pore volume was 0.8 cm^3 g^{-1}. The FT-IR spectrum of the empty host showed absorption bands for the surface hydroxy groups at 3430 cm^{-1}, the silica framework from 1100 to 600 cm^{-1}, and adsorbed H_2O at 1700 cm^{-1}.

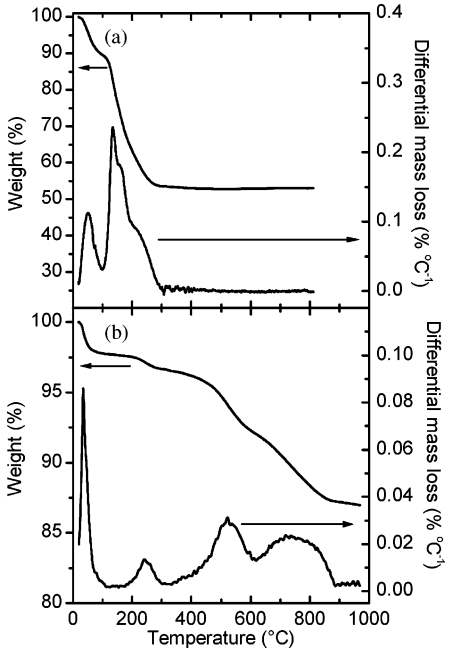

Figure 3. Thermogravimetric analysis of (a) TBAOH-treated MCM-41 and (b) PPV/MCM-41.

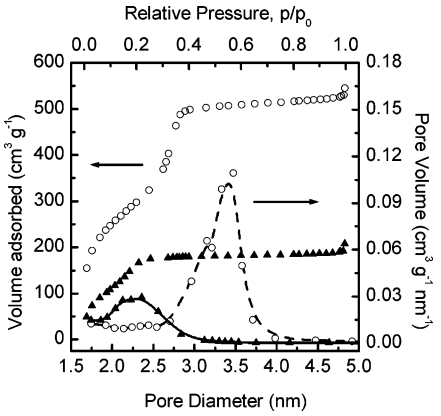

Figure 4. N_2 adsorption isotherms and derived BJH pore size distributions for MCM-41 (○) and TBAOH-treated MCM-41 (▲).

Following TBAOH treatment of MCM-41, TGA showed 10% H_2O content and a 38% mass loss between 100 and 300 °C; this was ascribed to the decomposition of the TBA counterion (Figure 3a). The mass content of TBA suggests that 15% of all Si atoms in the MCM-41 host were associated with a TBA counterion. The presence of the counterion reduced the BJH pore diameter by 1.2 nm (Figure 4). The polymerization step then yielded a bright green powder. Thermal conversion of the polymer under vacuum led to a fluorescent yellow powder.

TGA of the composite material (Figure 3b) showed an initial H_2O desorption at 40 °C, followed by a 1% weight loss at 250 °C, which is most likely due to residual TBA in the material that did not decompose during the thermal conversion process. The polymer degradation began at 350 °C and showed at least two different decomposition processes, at 525 °C and 730 °C. All samples showed a polymer content between 6 and 10

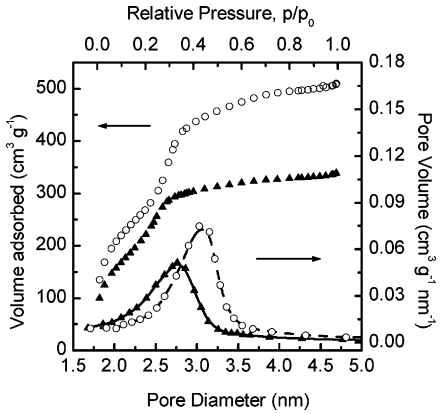

Figure 5. N_2 adsorption isotherms and BJH pore size distributions of MCM-41 (○) and PPV/MCM-41 (▲).

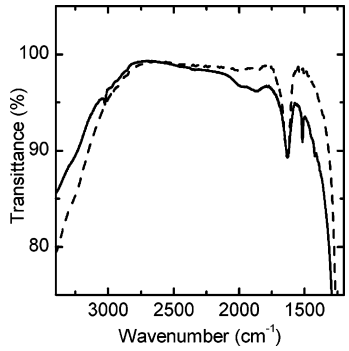

Figure 6. FT-IR transmission spectra of MCM-41 (dashes) and PPV/MCM-41 (solid).

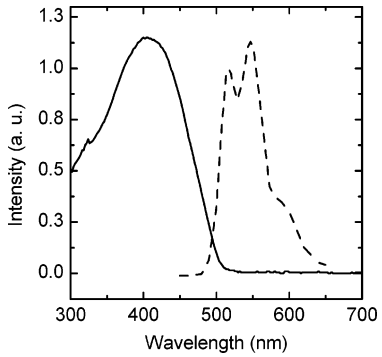

Figure 7. UV/Vis absorption spectrum (solid) and photoluminescence spectrum (dash) of PPV/MCM-41.

wt. %. Analysis of the N_2 adsorption isotherm (Figure 5) indicated a reduced BET surface area (8.5×10^2 m^2g^{-1}) and pore volume (0.51 cm^3 g^{-1}). The BJH pore diameter was observed to decrease by 0.2 to 0.3 nm.

The FT-IR spectrum of PPV/MCM-41 (Figure 6) showed new bands characteristic of PPV. The band at 3025 cm^{-1} is associated with the C−H stretch in *trans*-vinylene, while the bands at 1517 and 1422 cm^{-1} are due to 1,4-phenylene ring stretching modes.[41] The UV/Vis absorbance spectrum of the composite showed an onset at 500 nm (2.5 eV) and a peak at 420 nm (3 eV), while the photoluminescence spectrum showed peaks at 517, 547, and 590 nm (Figure 7), in agreement with the reported values for PPV.[42] The presence of PPV is

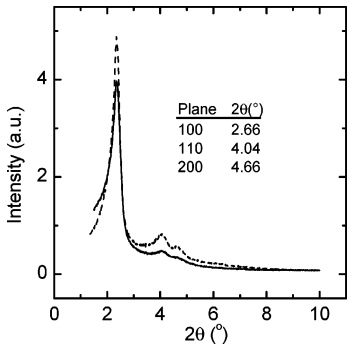

Figure 8. Powder X-ray diffraction pattern for MCM-41 (dash) and PPV/MCM-41 (solid).

Table 1. Parameters for Calculation of PPV Mass Fraction in Model PPV/MCM-41

property	value	source
PPV repeat length	0.66 nm	ref 45
PPV repeat unit mass	102.1 g mol^{-1}	
MCM-41 wall density	2.2 g cm^{-3}	amorphous SiO_2; ref 46
MCM-41 lattice constant	4.3 nm	X-ray diffraction
MCM-41 pore diameter	3.1 nm	N_2 physisorption

clearly indicated by these results. The central issue in the characterization of this material is whether the polymer chains actually reside in the channels of MCM-41, or instead form a thin layer on the outside of the host particles.

The X-ray diffraction data (Figure 8) indicated that the polymerized sample retained the overall order of the host material, with no substantial shift in the diffraction peak positions. No attempt was made to interpret the changes in the peak intensities.

The TGA data for PPV/MCM-41 (Figure 3b) clearly indicate that the thermal behavior of the polymer is altered from that in its unencapsulated form, which shows only one degradation process at 540 °C.[43] The higher-temperature degradation process at 730 °C has also been observed for PPV encapsulated in montmorillonite.[44] This strongly suggests the presence of some encapsulated polymer. It is possible that the lower degradation process is associated with the presence of some unencapsulated polymer.

A simple model for the composite material can be used to determine the approximate polymer mass content for a given number of polymer chains per channel in MCM-41. With the assumptions that (1) the polymer chains have no conformational defects, (2) they are oriented parallel to the channels, (3) the effect of end-groups can be ignored, and (4) the polymer on the external surface is minimal, the mass fraction F of polymer in MCM-41 for a given number of chains N per pore can be calculated, using parameters given in Table 1:

$$F = \frac{N \cdot 2.57}{190 + N \cdot 2.57}$$

(41) Papadimitrakopoulos, F.; Konstadinidis, K.; Miller, T. M.; Opila, R.; Chandross, E. A.; Galvin, M. E. *Chem. Mater.* **1994**, *6*, 1563.
(42) Samuel, I. D. W.; Crystall, B.; Rumbles, G.; Burn, P. L.; Holmes, A. B.; Friend, R. H. *Synth. Met.* **1993**, *54*, 281.
(43) Gagnon, D. R.; Capistran, J. D.; Karasz, F. E.; Lenz, R. W.; Antoun, S. *Polymer* **1987**, *28*, 567.
(44) Oriakhi, C. O.; Zhang, X. R.; Lerner, M. M. *Appl. Clay Sci.* **1999**, *15*, 109.
(45) Martens, J. H. F.; Bradley, D. D. C.; Burn, P. L.; Friend, R. H.; Holmes, A. B.; Marseglia, E. A. *Synth. Met.* **1991**, *41*, 301.
(46) Lide, D. R., Ed. *CRC Handbook of Chemistry and Physics*; 3rd Electronic Edition ed.; CRC Press: Boca Raton, FL, 2000.

Table 2. Polymer Mass Fraction *F* for *N* Polymer Chains Per Pore in MCM-41

N	1	2	4	6	8	10
F (%) ± 1%	1	3	5	8	10	12

Values of *F* for small values of *N* are given in Table 2. This shows that even one polymer chain per pore would represent a substantial mass loading of the sample. The experimental mass content of 8% suggests that the pores of MCM-41 contain 6 polymer chains each on average. If some of the polymer (∼50% as suggested by TGA) is assumed to be externally located, each channel contains 3 polymer chains on average.

The reduction of the BJH pore diameter of the composite material, albeit small, was observed reproducibly and is significant. The BJH method assumes a cylindrical geometry for the pores and does not provide any information about the arrangement of the polymer chains within the pores; one possible interpretation is that the polymer is present as a thin layer on the walls of the pores. As the PPV backbone is planar, a polymer chain can lie flat against the pore wall and produce a relatively small change in the BJH pore diameter. The observed differences in pore diameter reduction could suggest differences in polymer conformation within the pores, leading to a different effect on the isotherm. The small amount of residual TBA ions observed by TGA (1 wt. %) would be expected to reduce the BJH pore diameter by 0.03 nm, based on the effect of 38 wt. % TBA content.

If polymerization occurred strictly in solution, due to proton transfer from the solvent or trace H_2O and consequent migration of the basic species into the bulk solution, the polymer might be present strictly as a layer coating the outside of the MCM-41 particles. The effect on the N_2 adsorption isotherm would then be very different: if the pores were fully blocked, no substantial adsorption would occur. Partial blockage of the pores by a superficial layer would not alter the observed capillary condensation point, but would introduce hysteresis into the isotherm, which was not observed. An external layer that did not impede the adsorption process would not reduce the observed pore diameter, but would simply reduce the specific surface area and pore volume due to the presence of additional, nonporous mass in the sample. The relative decrease in the specific surface area (15%) and pore volume (36%) is greater than the additional mass (8%) and also in agreement with the relative decrease expected for a cylindrical geometry ($\Delta V/V = 2\ \Delta A/A$).

The distribution of polymer in the composite particles was investigated further by EELS and EFTEM. Normal TEM investigation did not show any substantial difference between the empty and polymerized samples. A substantial surface layer would have been visible as an amorphous (structure-free) layer at the particle edges. For 1 μm particles, an external polymer mass content of 4% would give rise to a uniform external layer of ∼7 nm (assuming a polymer density of 1 g cm^{-3}). In addition, no bulk polymer particles were observed by TEM. The low loss spectra of the empty and polymer-filled MCM-41 are compared in Figure 9. The zero-loss peak has been removed by careful subtraction of a reference peak, revealing that only PPV/MCM-41 has

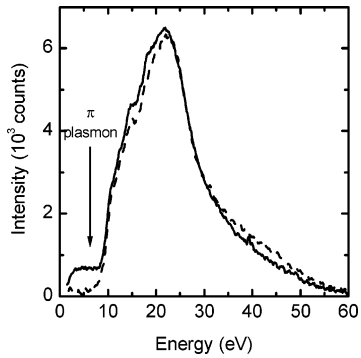

Figure 9. Electron energy-loss spectrum of MCM-41 (dash) and PPV/MCM-41 (solid).

losses below 8 eV. These may be assigned to the aromatic $\pi-\pi^*$ plasmon at 6−7 eV, and to optical absorption of the conjugated chain below 5 eV. At energies above 8 eV, the spectra are dominated by the broad bulk plasmon of the silica matrix centered at 22 eV, in agreement with the value observed for a form of mesoporous silica.[47] The polymer bulk plasmon would be expected to appear at a similar energy[48] and could not be distinguished. The shoulders visible between 10 and 20 eV are most likely due to weak surface plasmons. The stability of the material seemed very good under a diffuse beam without any special measures taken to limit beam damage.

Energy filtering on the $\pi-\pi^*$ plasmon is experimentally most practical as the tail of the zero-loss peak is substantial below 5 eV. The images filtered at 0, 6, and 12 eV are shown in Figure 10. As expected from the loss spectra, the 6 eV images are most revealing: empty MCM-41 does not show substantial losses in this range, and the image is correspondingly dark. The 6 eV image of PPV/MCM-41 shows losses distributed throughout the particle. Intensity variations are seen, and these are due to thickness variations of the sample, as seen in the 0 eV image. There is no indication of edge brightness, which would have suggested the presence of a thin polymer coating on the outside of the particles. The periodicity of the host material is also visible. Although this structure is not fully resolved, it strongly suggests that the polymer is confined in the channels. This periodic structure could be due to thickness variations in the sample, but this can be effectively ruled out by reference to the 6 eV image of empty MCM-41, which shows no structure whatsoever. A line analysis of the 6 eV images of PPV/MCM-41 clearly shows the resolved periodic structure (Figure 11). The lacey carbon support in Figure 10a also shows strong losses at 6 eV. The 12 eV image is not affected visibly by the presence of PPV. These results corroborate the physisorption and TGA data in suggesting that the polymer chains are incorporated into the channels of MCM-41. Although the presence of some external polymer may be indicated by the TGA data, the EFTEM results indicate that this can only be in the form of a very thin layer (< 2 nm), corresponding to < 1 wt. % external polymer.

(47) Yin, J. S.; Wang, Z. L. *Appl. Phys. Lett.* **1999**, *74*, 2629.
(48) Egerton, R. F. *Electron Energy-Loss Spectroscopy in the Electron Microscope*; 2nd ed.; Plenum Press: New York, 1996.

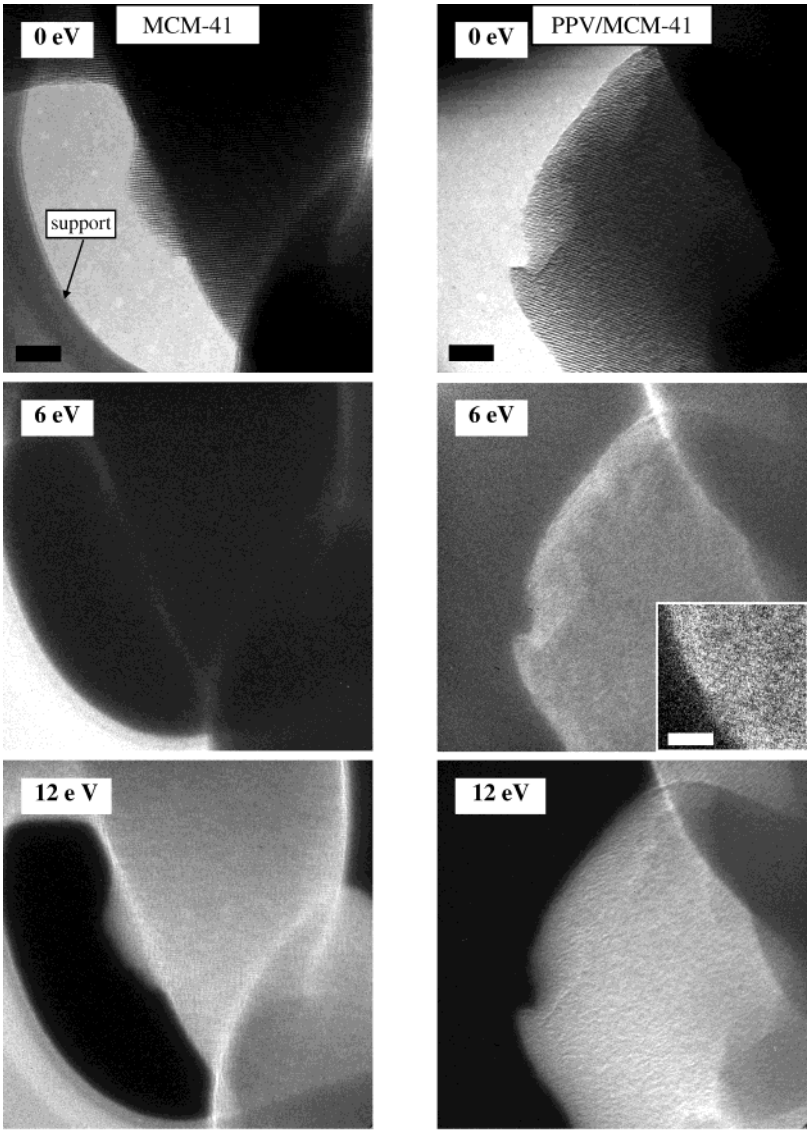

Figure 10. EFTEM images for (a) MCM-41 and (b) PPV/MCM-41, filtered with a 2 eV window. The contrast has been enhanced on the inset. The main scale bar is 50 nm and the inset scale bar is 20 nm.

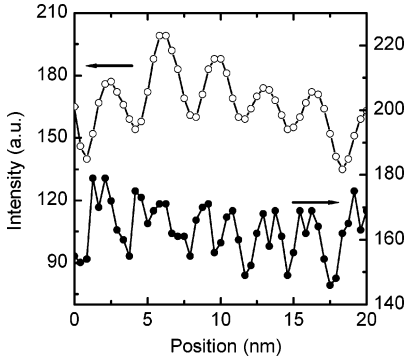

Figure 11. Intensity plot from 0 eV (○) and 6 eV (●) filtered images over a short line, on different areas of the sample.

Conclusions

A PPV/MCM-41 composite was synthesized using an in situ polymerization approach. N_2 physisorption and TGA supported polymer encapsulation in the pores of the host material. The polymer mass content suggested that an average of 3−6 polymer chains resided in each pore. The PPV distribution was determined unambiguously using chemical analysis by EELS and EFTEM, the first time this method has been used to demonstrate the inclusion of an organic host in porous MCM-41.

This demonstrates the ability of EFTEM to reveal directly the presence of conjugated polymer at very high resolution. The previous estimate of the resolution limit for mapping small conjugated molecules was based on the edge sharpness of a molecular crystal,[34] whereas these results show directly that such high resolution is achievable in a two-component material. Furthermore, EFTEM was used to visualize directly the presence of an organic guest in the channels of MCM-41 for the first time. The low number of polymer chains per pore also suggests that it may be possible to image a single isolated conjugated polymer chain (perhaps dispersed in a nonconjugated polymeric matrix) by this technique.

EFTEM is a unique tool for investigating composite materials, and is particularly suited for characterizing conjugated molecules on the nanometer scale. With more sophisticated treatment of the energy-filtered

images, it should be possible to determine the distribution of conjugated molecules and polymers in blends, which are very important in molecule-based photovoltaic and light-emitting devices.[49−51]

Acknowledgment. We thank Gianluigi Botton for initial help with the TEM and EELS, the Simon Fraser University Nano-Imaging Facility for access to their TEM, and the Natural Sciences and Engineering Research Council of Canada for support of this research.

CM035303H

(49) Sariciftci, N. S. *Prog. Quantum Electron.* **1995**, *19*, 131.
(50) Moons, E. *J. Phys.: Condens. Matter* **2002**, *14*, 12235.
(51) Chappell, J.; Lidzey, D. G.; Jukes, P. C.; Higgins, A. M.; Thompson, R. L. O.; Connor, S.; Grizzi, I.; Fletcher, R. O.; Brien, J.; Geoghegan, M.; Jones, R. A. L. *Nat. Mater.* **2003**, *2*, 616.